DTU Library

A novel temperature control method for shortening thermal cycling time to achieve rapid polymerase chain reaction (PCR) in a disposable polymer microfluidic device.

Bu, Minqiang; R. Perch-Nielsen, Ivan; Jørgensen, Karen Skotte; Skov, Julia ; Sun, Yi; Bang, Dang Duong; E. Pedersen, Michael ; Hansen, Mikkel Fougt; Wolff, Anders

Link back to DTU Orbit

A NOVEL TEMPERATURE CONTROL METHOD FOR SHORTENING THERMAL CYCLING TIME TO ACHIEVE RAPID POLYMERASE CHAIN REACTION (PCR) IN A DISPOSABLE POLYMER MICROFLUIDIC DEVICE

M. Bu[1,2], I. R. Perch-Nielsen[2], K. S. Sørensen[1,2], J. Skov[2], Y. Sun[1],
D. D. Bang[3], M. E. Pedersen[2], M. F. Hansen[1], A. Wolff[1]

[1]Technical University of Denmark, DTU Nanotech, DK-2800 Kgs. Lyngby, Denmark
[2]DELTA, Venlighedsvej 4, DK-2970 Hørsholm, Denmark
[3]Technical University of Denmark, National Food Institute, DK-2860 Søborg, Denmark

Abstract — **We present a new temperature control method capable of effectively shortening the thermal cycling time of polymerase chain reaction (PCR) in a disposable polymer microfluidic device with external heater and temperature sensor. The method employs optimized temperature overshooting and under-shooting steps to achieve a rapid ramping between the temperature steps for DNA denaturation, annealing and extension. The temperature dynamics within the microfluidic PCR chamber was characterized and the overshooting and undershooting parameters were optimized using the temperature dependent fluorescence signal from Rhodamine B. The method was validated with PCR amplification of *mecA* gene (162 bp) from Methicillin-resistant *Staphylococcus aureus* bacterium (MRSA), where the time for 30 cycles was reduced from 50 min (without over- and undershooting) to 20 min.**

Keywords: **Temperature control method, Polymerase chain reaction (PCR), Polymer microfluidic device**

I - Introduction

With the potential of low cost, rapid reaction and multi-functional integration, microfluidic devices using PCR for nucleic acid analysis have been extensively exploited for a wide range of applications [1-2], such as pathogen sensing [3] and point-of-care diagnostics [4-5].

Using silicon microfabrication technology, ultra fast real-time PCR has been achieved with 40 cycles in less than 6 minutes [6]. However, the high cost of the microfabrication process hindered commercialization of this type of microfluidic device. Low-cost fabrication technologies, such as injection moulding, have been used recently to fabricate disposable polymer microfluidic devices for DNA analysis [7].

In comparison to the silicon, polymer materials have 1000 times lower thermal conductivity, which substantially slows down the heat transfer, especially when external heaters are used to heat the reaction chamber. This considerably prolongs the time for PCR cycling. However, by optimizing the heating and cooling control, a rapid PCR is still achievable, even in polymer microfluidic devices with external heaters.

In this work, we present a new method featuring temperature overshooting for heating and undershooting for cooling to obtain a rapid ramping between the three temperature steps for PCR. The work is part of a microfluidic control platform with a re-usable micro-pump/valve actuator [8] and a re-usable external silicon heater for DNA sample preparation and PCR amplification in a disposable microfluidic TOPAS® cyclic olefin copolymer chip for rapid pathogen detection.

II– Experimental

A. Design of PCR Thermal Cycling Platform

Figure 1a illustrates the design of PCR thermal cycling platform. An external silicon heater (10 mm × 13 mm × 0.35 mm) with integrated Pt thin film resistive heater and temperature sensor on the bottom side is used to control the temperature in the PCR reaction chamber of an injection moulded TOPAS® chip (Figure 1b). The silicon heater is mounted on a printed circuit board (PCB) with conductive silver epoxy glue, and the PCB is mounted in a recess machined in an aluminium plate.
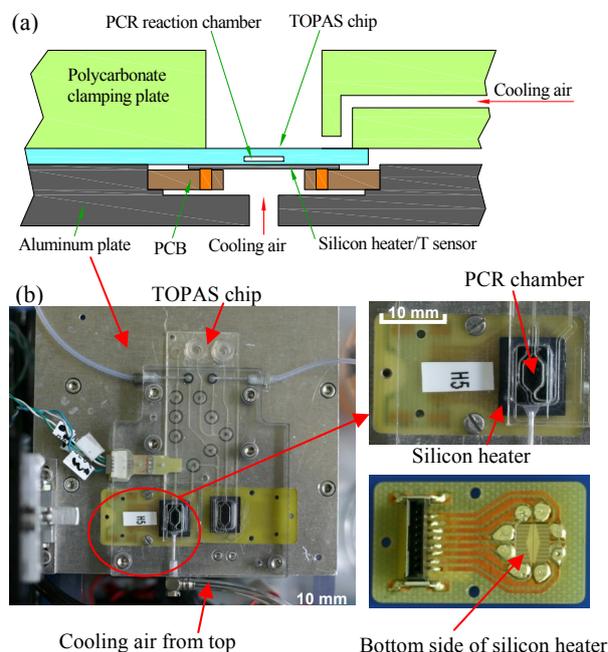

Figure 1*: An illustration (a) and a top view (b) of the thermal cycling platform.*

The disposable TOPAS® chip is clamped under a polycarbonate clamping plate. The clamping plate has a hole above the PCR chamber through which compressed air (3.5 bar, 22 ºC) can be passed to cool the top of the TOPAS® chip during PCR. Compressed air is

also used to cool the silicon heater from bottom of the platform. Figure 1b shows a top view of the thermal cycling platform and a silicon heater (top and bottom view). The PCR chamber in the injection moulded TOPAS® chip (1 mm thick) is sealed with a TOPAS® film (250 μm thick) using ultrasonic welding. The reaction chamber has a dimension (depth×width×length) of approximately $0.4 \times 3.4 \times 5$ mm^3 (~6 μL).

B. Steady-State On-Chip Temperature Measurement

Since the temperature sensor is integrated on the external heater, but not in the chip, non-contact methods were used to characterize the temperature in the PCR chamber. An infrared (IR) camera was used to monitor the steady-state temperature on the top surface of the TOPAS® chip (T_{top}), when heater temperatures (T_{heat}) was changed from 50 to 100 ºC with a step of 10 ºC. At each step, to ensure the system reaches thermal equilibrium, the heater was kept at each set temperature for 15 minutes before T_{top} was measured.

In order to characterize the temperature in the PCR chamber (T_{cham}), measurement on the melting points of PCR amplicons of different lengths has been carried out both on-chip and in a conventional real-time PCR machine (Chromo4, Bio-Rad, Denmark) as a reference (T_m). PCR amplicons were amplified in the conventional PCR machine first and then filled into the TOPAS® chips. When the DNA fragments melt in the TOPAS® chip, $T_m = T_{cham}$, and the heater temperature at this moment was marked as $T_{m,heater}$. During the measurement, T_{heat} was changed in steps of 0.2 ºC with a dwell time of 32 s at each step. No difference was found between sweeping up and down in temperature, indicating that the dwell time was sufficiently long to reach thermal equilibrium. The amplicons used were: (1) PVL gene of MRSA (83 bp, T_m=78 °C); (2) *mecA* gene of MRSA (162 bp, T_m=78.8 °C); (3) Hiporicase gene of *Campylobacter jejuni* (150 bp, T_m=79.3 °C); (4) *spa* gene of MRSA (400 bp, T_m=84.4 °C); (5) 16S RNA gene of *Campylobacter* (300 bp, T_m=86.4 °C).

C. Dynamic On-Chip Temperature Measurements

The temperature dynamics within the PCR chamber was monitored in real-time using the temperature dependent fluorescence signal from a 25 μM Rhodamine B (RhB) solution in the chamber. The fluorescence of RhB decreases as a function of increasing temperature. The intensity was converted to temperature using a three point calibration based on a comparison between steady-state fluorescence signals and steady-state temperatures in the chamber obtained from a 1-dimensional thermal model of the system.

D. Temperature Over- and Undershooting Method and its Validation

The characterization of the dynamic response of the temperature in the chamber was employed to optimize

the setting of T_{heat} in this new temperature control method for PCR. This method features a step with temperature overshooting of several degrees above the target set point for the extension and denaturing steps, as well as a step with temperature undershooting below the target temperature set point for the denaturing step.

The optimized temperature over- and undershooting method was validated with the on-chip PCR amplification of the *mecA* gene of MRSA.

III – Results and Discussion

A. Steady-State On-Chip Temperature Measurement

Figure 2 shows the IR camera measured steady-state temperature T_{top} as a function of the heater temperature T_{heat}. It also shows the reference melting temperatures T_m (=T_{cham}) as function of the $T_{m,heater}$ for the five studied PCR amplicons.
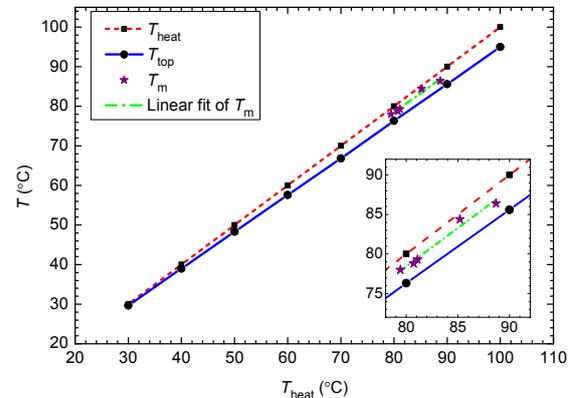

Figure 2: *Temperature of chip top T_{top} and DNA reference melting temperatures T_m vs. heater temperature T_{heat}.*

From Figure 2 it is seen that T_{top} systematically lies below T_{heat} with a difference that increases linearly with increasing T_{heat} (e.g. 5 ºC when T_{heat} = 100 ºC). This is in agreement with the expectations from a 1D thermal circuit model of the system and also shows that the largest temperature gradient occurs between the top surface of the chip and the surroundings. The values of T_m (T_{cham}) vs. $T_{m,heater}$, as expected, lie systematically between T_{top} and T_{heat} and are approximately linearly related to T_{heat}. These values provide an independent calibration of the temperature in the PCR chamber and it is found (in agreement with expectations from modelling) that near the investigated melting temperatures, T_{cham} is about 1.6 ºC lower than the heater temperature T_{heat}, when $T_{heat} \approx 85$ ºC.

We further tested the reproducibility of on-chip measurements of melting points when the measurements were carried out in different chips. The variability in measurements from chip to chip may originate from chip fabrication variations and the quality of the thermal contact to the chip. Figure 3 shows the on-chip melting curves obtained from six different chips containing PCR amplicons of the PVL gene of MRSA (83 bp, T_m=78 °C). The chips were prepared with identical procedures and the experiments were carried out under identical conditions.
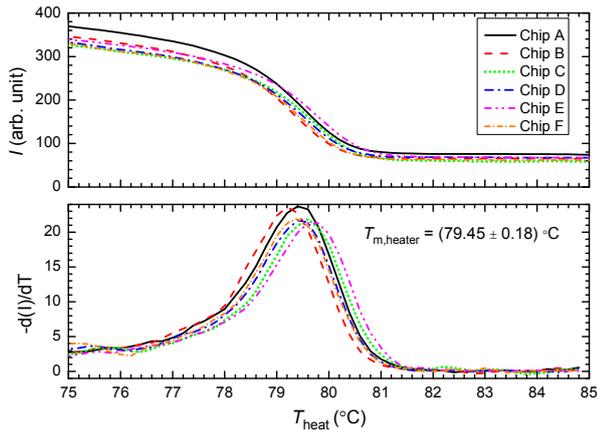
Figure 3: *Melting curve analysis of PCR amplicon of PVL gene from MRSA in 6 different TOPAS chips. Top: Fluorescence intensity (I) drops substantially at melting point. Bottom: Negative first derivative of the fluorescence intensity shows the on-chip measured melting point ($T_{m,heater}$).*

From the measurements, we obtain $T_{m,heater}$ = 79.45 ºC with a standard deviation of 0.18 ºC. The value of $T_{m,heater}$ is about 1.5 ºC higher than the reference value of T_m as expected due to the temperature drop between the heater and the PCR chamber. The standard deviation of only 0.18 ºC on the melting point demonstrates a very good reproducibility in chip fabrication and mounting. A small variable gap between the chip bottom and the heater would have a significant impact on the variation of the obtained values. This indicates that a reproducible thermal contact and an efficient heat transfer to the disposable TOPAS® chip through the bottom of the chip have been obtained in this system.

B. Dynamic On-Chip Temperature Measurement and Optimization of Under- and Overshooting Method

Dynamic on-chip measurements of T_{cham} and the optimization of temperature under- and overshooting for the PCR amplification of *Campylobacter* DNA (150 bp and 300 bp) were carried out. The optimal values of T_{heat} for these steps were found using a commercial PCR machine and the corrections based on Figure 2 to 54.5 ºC, 73 ºC and 96.5 ºC, respectively.

Figure 4 shows the dynamic on-chip temperature measurements results obtained using Rhodamine B fluorescence for the three temperature steps required to carry out the PCR cycling. The measured Rhodamine B fluorescence signal (F_N) was normalized to the value when the chamber reaches thermal equilibrium. When no over- or undershooting is used, the PCR chamber is not able to reach thermal equilibrium in 25-30 s of dwell time. This is due to the low thermal conductivity of the polymer and the significant thermal mass of the chip.

To decrease the time required to reach thermal equilibrium in the PCR chamber, we systematically investigated controlled temperature over- and undershooting, where a higher or lower value of T_{heat} is used for a fixed period of time of 3 s. Figure 4 shows the results of these investigations for different values of the over- and undershooting temperatures. The optimal parameters of over- and undershooting temperatures for three steps in PCR are: 3 s at 90 ºC (annealing to extension), 3 s at 110 ºC (extension to denaturing) and 3 s at 45 ºC (denaturing to annealing). These choices results in minimal overshooting of the temperature in the PCR chamber and shortens the time required to attain thermal equilibrium at each temperature step to 5-10 s. This optimization procedure can easily be used to optimize the over- and undershooting parameters for other PCR protocols.
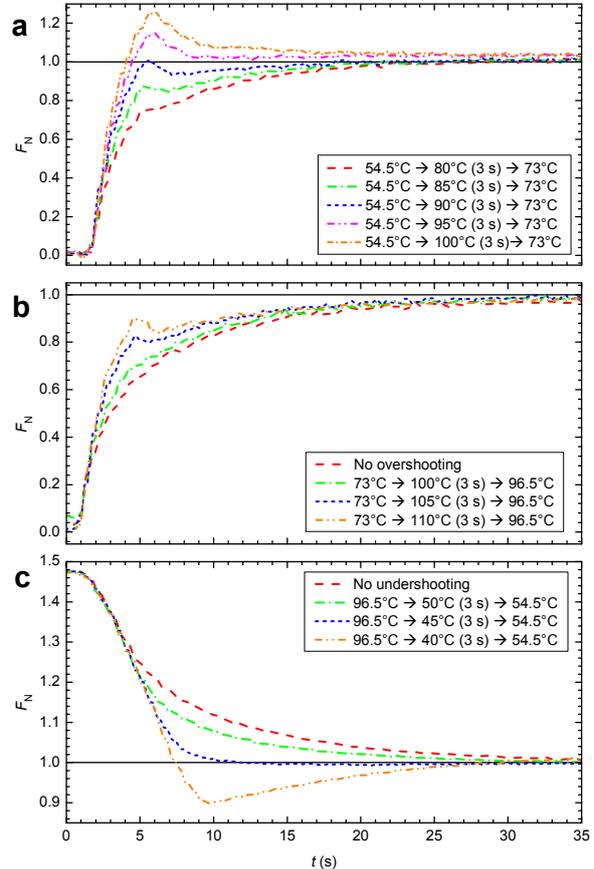

Figure 4: *Rhodamine B fluorescence signal (F_N) for optimization of (a) overshooting from 54.5 °C (annealing step) to 73 °C (extension step), (b) from 73 °C to 96.5 °C (denaturing step), and (c) undershooting from 96.5 °C to 54.5 °C.*

C. Validation of Over- and Undershooting Method and Optimization of PCR Protocol

When the parameters for temperature over- and undershooting are determined, the dwell time at each temperature have to be optimized to obtain the shortest acceptable cycle time for on-chip PCR.

Different combination of dwell time for the both the over- and undershooting temperature as well as for the annealing, extension and denaturation step have been investigated for the real-time PCR amplification of *mecA* Gene of MRSA. Five experiments (PCR 01 – PCR 05) have been conducted in five different chips using the values for temperature levels and dwell time given in Table 1. The recorded ramping time for the silicon heater to reach its set point from the previous step to the next step is given in parentheses.

	T_{heat} [°C]	PCR 01/02 [s]	PCR 03 [s]	PCR 04 [s]	PCR 05 [s]
Initial activation step	110	6	6	6	6
	95.5	182	182	182	182
Annealing	52	5 (1.9)	5 (1.9)	5 (1.9)	3 (1.9)
	60	22 (0.8)	12 (0.8)	7 (0.8)	4 (0.8)
Extension	81	5 (0.2)	5 (0.2)	5 (0.2)	3 (0.2)
	73	22 (0.6)	12 (0.6)	7 (0.6)	4 (0.6)
Denatura-tion	108	5 (0.5)	5 (0.5)	5 (0.5)	3 (0.5)
	95.5	22 (0.6)	12 (0.6)	7 (0.6)	4 (0.6)
Cycle time [s]		85.6	55.6	40.6	25.6

Figure 5 shows the dynamic temperature response of the heater and PCR chamber for the PCR 04 conditions in Table 1. For the heater, the heating and cooling rates are approximately 14 ºC/s and 9 ºC/s, respectively, and for the PCR chamber heating and cooling rates of about 4.3 ºC/s and 5 ºC/s are achieved.
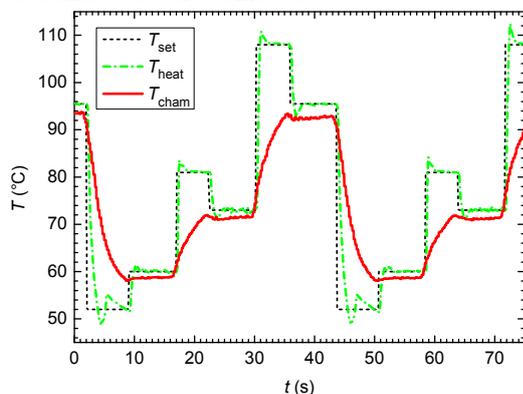

Figure 5: *The dynamic temperature response of the on-chip PCR chamber using optimized over- and undershooting parameters (PCR 04). The temperature in the PCR chamber is measured as described in section II.B.*
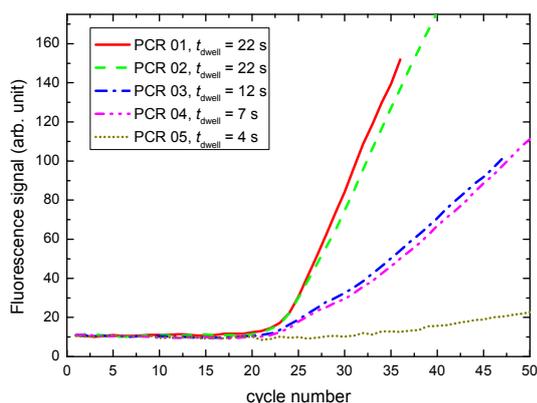

Figure 6: *Fluorescence signal of real-time PCR with the indicated dwell time (t_{dwell}) at each step. The cycle time for PCR 05 is too short to achieve an acceptable PCR analysis.*

Figure 6 shows measured real-time PCR fluorescence intensity vs. cycle number for the conditions in Table 1. The figure indicates that the *mecA* gene is amplified efficiently with a relatively high yield for conditions PCR 01 to PCR 04, where PCR 04 has the

shortest total run time of about 20 min for 30 cycles. The identity of the PCR product was verified by gel electrophoresis (Figure 7). Without temperature over- and undershooting a total run time of 50 min for 30 PCR cycles is required for efficient amplification.
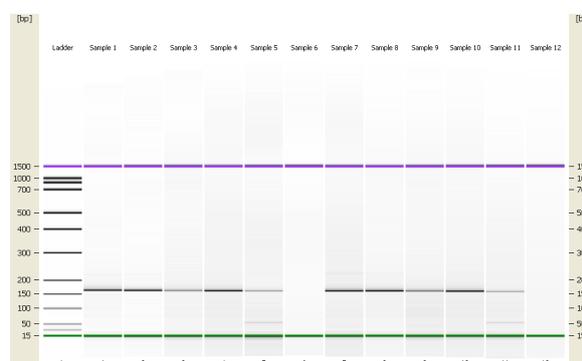

Figure 7: *Gel electrophoresis analysis of 5 PCR amplicons reveals the successful amplification of specific mecA gene of MRSA. From left to right, lane L: ladder, lane 1-5: PCR 01-05, lane 6: empty, lane 7-11: repeat of PCR 01-05, lane 12: empty. The size of the product is 162 bp.*

IV - Conclusion

An overshooting and undershooting control method has been investigated and carefully optimized to obtain a rapid temperature ramping during PCR on a disposable polymer chip using external heaters. The experimental results proved that this method is able to effectively shorten the PCR thermal cycling time in the investigated polymer chip by ~50%, compared to PCR setting without over/undershooting in the same chip.

V – Acknowledgements

References

[1] P.-A. Auroux, Y. Koc, A. deMello, A. Manz and P. J. R. Day, *Lab Chip* **4**, pp.534–546, 2004.

[2] Y. Zhang, P. Ozdemir, *Anal. Chim. Acta* **638**, pp. 115-125, 2009.

[3] J. Mairhofer, K. Roppert, P. Ertl, *Sensors* **9**, pp. 4804-4823, 2009.

[4] V. Gubala, L. F. Harris, A. J. Ricco, M. X. Tan and D. E. Williams, *Anal. Chem.* **84**, pp 487–515, 2012.

[5] L. Gervais, N. de Rooij and E. Delamaeche, *Advanced Materials* **23**, H151-H176, 2011.

[6] P. Neuzil, C. Zhang, J. Pipper, S. Oh and L. Zhuo, Nucleic Acids Research **34**(11), e77, 2006.

[7] Y. Sun, Y. C. Kwok, *Anal. Chim. Acta* **556**, pp.80-96, 2006.

[8] M. Bu, I. R. Perch-Nielsen, Y. Sun and A. Wolff *Proc. 16th Int. Conf. on Solid-State Sensors, Actuators and Microsystems (Transducers'11),* Beijing, China, June 5-9, 2011, pp 1244-1247.